

# Experimental investigations of a robust control strategy applied to cultures of *S. cerevisiae*

Laurent Dewasme, Frederic Renard and Alain Vande Wouwer

**Abstract**—In this paper, two robust RST control schemes for the regulation of either the ethanol concentration or the dissolved oxygen concentration in cultures of *S. cerevisiae* are presented and illustrated with various simulation and experimental results. Both controllers only require the prior knowledge about one stoichiometric coefficient and only one on-line measurement signal, making them easily implementable in an industrial environment. Disturbance rejection is ensured thanks to an on-line parameter adaptation procedure, which delivers as a side product an estimate of the growth rate that can be used for process monitoring purposes. The robustification of the controllers is achieved in a simple way, using the observer polynomial. Additional issues, such as the presence of a delay in the system response (as observed in real-life experiments) or non negligible sensor dynamics, are also addressed.

## I. INTRODUCTION

*S. cerevisiae* is one of the most popular host microorganism for vaccine production. The possibility to easily express a variety of different recombinant proteins explains its important role in the pharmaceutical industry. In order to maximize productivity, a common strategy is to regulate the ethanol concentration at a low value, thus ensuring an operating point close to the edge between the respirative and respiro-fermentative regimes where the yeast respirative capacity is exactly filled (bottleneck assumption of Sonnleitner's model [1]). Several applications of this principle can be found, for instance in [2], [3], [4], [5], [6], [7]. However, these control schemes all require the on-line measurement of the ethanol concentration, implying the availability of an (unfortunately quite expensive) ethanol probe. This explains that alternative strategies based on more basic measurement signals, such as the dissolved oxygen concentration, have been proposed, e.g. in [8], [9], or that software sensors reconstructing ethanol from the measurements of basic signals have been designed [10].

In a recent study led by the same authors [7], a RST controller with Youla parametrization is developed for the regulation of the ethanol concentration and tested successfully in real-life experiments. One of the main advantage of this approach is that it is based on a simple linear model linking the feed flow rate to the ethanol concentration, and a simple linear model of the disturbance, which represents the substrate demand for cell growth. The prior knowledge of only one stoichiometric coefficient is required, whereas the apparent growth rate can be easily estimated on-line (in order to ensure a good disturbance rejection).

L. Dewasme, F. Renard and A. Vande Wouwer are with Service d'Automatique, Faculté Polytechnique de Mons, 7000 Mons, Belgium, Laurent.Dewasme; Alain.VandeWouwer@fpm.s.ac.be

The objective of the present study is to propose an alternative, simpler, controller design based on the observer polynomial, and to consider both the ethanol regulation and the dissolved oxygen regulation problems. Several additional issues are also addressed, including the presence of a delay in the system response (as observed experimentally), and the influence of the probe dynamics when using relatively fast sampling. Finally, new experimental results are discussed, which illustrate the performance of the proposed scheme in various conditions.

This paper is organized as follows. The next section introduces the nonlinear model of Sonnleitner [1] and, using the singular perturbation principle, derives two linear models linking either the feed flow rate to the ethanol concentration or the dissolved oxygen concentration. The controller design and the on-line parameter adaptation are presented in Section 3. Section 4 discusses several simulation results demonstrating the efficiency of the proposed control strategy, whereas Section 5 illustrates the performance of the ethanol regulation in a series of real-life experiments. The last section is devoted to general conclusions and comments.

## II. MODELING YEAST FED-BATCH CULTURES

### A. Nonlinear dynamic model

The kinetic model considered in this study is based on Sonnleitner's bottleneck assumption [1]. During a culture, the yeast cells are likely to change their metabolism because of their limited oxidative capacity. When glucose is in excess (concentration  $S > S_{crit}$ ), the yeast cells produce ethanol through fermentation, and the culture is said in respiro-fermentative (RF) regime. On the other hand, when glucose becomes limiting (concentration  $S < S_{crit}$ ), the available glucose, and possibly ethanol (as a substitute carbon source), if present in the culture medium, are oxydized. The culture is then said in respirative (R) regime.

Component-wise mass balances give the following equations :

$$\frac{d(VX)}{dt} = (k_1r_1 + k_2r_2 + k_3r_3)XV - DVX \quad (1a)$$

$$\frac{d(VS)}{dt} = -(r_1 + r_2)XV + F_{in}S_{in} - DVS \quad (1b)$$

$$\frac{d(VE)}{dt} = (k_4r_2 - r_3)XV - DVE \quad (1c)$$

$$\frac{d(VO)}{dt} = -(k_5r_1 + k_6r_3)XV - DVO + VOTR \quad (1d)$$

$$\frac{dV}{dt} = F_{in} \quad (1e)$$

where X, S, E and O are, respectively, the concentration in the culture medium of biomass, glucose, ethanol and dissolved oxygen,  $k_i$  are the yield coefficients,  $S_{in}$  is the substrate concentration in the feed,  $F_{in}$  is the inlet feed rate,  $V$  is the culture medium volume and  $D$  is the dilution rate ( $D = F_{in}/V$ ).  $r_1$ ,  $r_2$  and  $r_3$  are the reactions rates defined in [7] as nonlinear functions of the elements concentrations in the culture medium. OTR represents the oxygen transfer rate from the gas phase to the liquid phase. A classical model of OTR is given by :

$$OTR = k_L a (O_{sat} - O) \quad (2)$$

where  $k_L a$  is the volumetric transfer coefficient and  $O_{sat}$  the dissolved oxygen concentration at saturation.

### B. Linear model of the dissolved oxygen evolution

The nonlinear model (1) is now linearized around a trajectory, using the singular perturbation principle. The idea here is to assume that the glucose dynamics is very fast, i.e., there is no accumulation of glucose in the culture medium as it is instantaneously consumed by the cells. Note that this assumption is certainly valid most of the time during a standard industrial fed-batch culture, but not at the early stage where the culture starts from the initial inoculum. This will result in some model discrepancy, requiring some kind of controller robustification.

Anyway, this assumption is the basis to build a first linear model linking the oxygen concentration to the substrate feed rate. If we define the glucose and the oxygen consumption rates :

$$q_S = r_1 + r_2 \quad (3a)$$

$$q_O = k_5 r_1 + k_6 r_3 \quad (3b)$$

we obtain from (1b) :

$$\frac{d(VS)}{dt} \approx 0 \quad \Rightarrow \quad X = \frac{F_{in} S_{in}}{q_S V} \quad (4)$$

Combining this last expression with (1d), we get :

$$\frac{dO}{dt} = -\left(\frac{q_O}{q_S} S_{in} + O\right) \frac{F_{in}}{V} + k_L a (O_{sat} - O) \quad (5)$$

The nominal trajectory around which the model is linearized is defined by  $F_{in}^*(t)$ ,  $V^*(t)$  so that  $O^*(t) = O_{ref}$  represents the oxygen setpoint.

The ratio  $\frac{q_O}{q_S}$  can be considered as a constant equal to  $k_5$  (considering only respiration on glucose in which case  $r_2 = 0$  and  $r_3 = 0$  in (3a) and (3b)). The dilution profile is obtained by considering  $O^*(t) = O_{ref}$  in (5) :

$$D^* = \frac{F_{in}^*}{V^*} = \frac{OTR^*}{k_5 S_{in} + O^*} \quad (6)$$

which is constant.

If the variation of the culture volume is neglected, a Taylor series expansion limited to the first order around the nominal trajectory allows to write :

TABLE I

PARAMETERS OF THE LINEAR DISCRETE MODELS (11A, 11B, 13A AND 13B).

	Oxygen Model	Ethanol Model	
		RF regime	R regime
a	$\exp(-k_L a T_s)$	1	1
b	$\frac{1}{k_L a} \frac{k_5 S_{in} + O^*}{V^*} (1 - a)$	$T_s \frac{k_4 S_{in} - E^*}{V^*}$	$T_s \frac{\frac{k_5}{k_6} S_{in} - E^*}{V^*}$
c	$V_0 (1 - \gamma)$	$\frac{k_4 r_1^*}{k_4 S_{in} - E^*} V_0 X_0$	$\frac{\frac{r_{Omax}}{k_6}}{\frac{k_5}{k_6} S_{in} - E^*}$
$\gamma$	$\exp(D^* T_s)$	$\exp(\mu T_s)$	$\exp(\mu T_s)$

$$\frac{d\delta O}{dt} = -\frac{k_5 S_{in} + O^*}{V^*} \delta F_{in} - (k_L a + D^*) \delta O \quad (7)$$

and, assuming that the dilution rate is negligible in comparison with  $k_L a$  :

$$\frac{d\delta O}{dt} = -\frac{k_5 S_{in} + O^*}{V^*} \delta F_{in} - k_L a \delta O \quad (8)$$

with  $\delta O = O - O^*$  and  $\delta F_{in} = F_{in} - F_{in}^*$

The integration of (1e) provides the expression of  $F_{in}^*(t)$  :

$$F_{in}^*(t) = D^* V_0 \exp(D^* t) \quad (9)$$

Replacing  $F_{in}^*$  by (9), we obtain the Laplace transform of (8) :

$$O(p) = -\frac{\frac{1}{k_L a} \frac{k_5 S_{in} + O^*}{V^*}}{1 + \frac{1}{k_L a} p} [F_{in}(p) - d_i(p)] \quad (10a)$$

$$d_i(p) = \frac{D^* V_0}{p - D^*} \quad (10b)$$

Finally, the discrete linear model is then given by :

$$O(k) = -\frac{b q^{-1}}{1 - a q^{-1}} [F_{in}(k) - d_i(k)] \quad (11a)$$

$$d_i(k) = \frac{c}{1 - \gamma q^{-1}} \delta(k) \quad (11b)$$

where the values of the parameters a, b, c and  $\gamma$  are presented in the first column of Table I.

$\delta(k)$  represents the unitary pulse,  $T_s$  is the sampling period and  $q^{-1}$  is the backward shift operator.

### C. Linear model of the ethanol evolution

In [11], it is demonstrated that the optimal operating point maximizing the biomass productivity corresponds to the edge between the respirative and respiro-fermentative regimes, where  $S = S_{crit}$  and ethanol is neither produced nor consumed. Regulating the ethanol concentration at a low setpoint allows therefore to bring the system close to this optimum. Considering assumption (4), we obtain from (1b) :

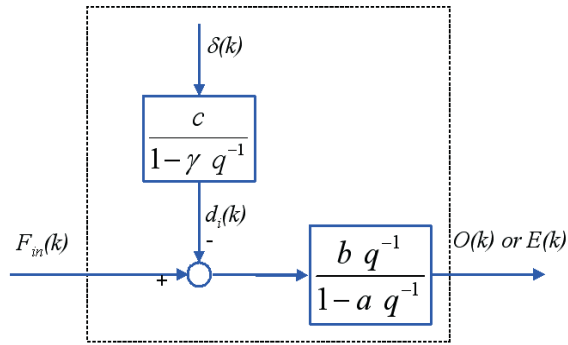


Fig. 1. Block diagram representation of the three simplified bioreactor linear models.

$$\frac{d(VS)}{dt} \approx 0 \quad \Rightarrow \quad r_2 X V = F_{in} S_{in} - r_1 X V \quad (12)$$

Inserting this last expression into (1c) and using a Taylor series expansion along the optimal trajectory (which now corresponds to  $E^*(t) = E_{ref}$ ), a discrete transfer function linking the ethanol concentration to the feed rate can be obtained for both the respirative and respiro-fermentative regimes :

$$E(k) = \frac{b q^{-1}}{1 - q^{-1}} [F_{in}(k) - d_i(k)] \quad (13a)$$

$$d_i(k) = \frac{c}{1 - \gamma q^{-1}} \delta(k) \quad (13b)$$

where the parameters  $b$  and  $c$  are functions of the operating regime. Their values are listed in Table I. In this particular case,  $a = 1$ . The parameter  $\mu$  present in the expression of  $\gamma$  is the cells specific growth rate.

Fig. 1 shows a block diagram subsuming the different linear models obtained so far. The variations of  $O(k)$  or  $E(k)$  depends on the difference between the feed rate  $F_{in}(k)$  and the disturbance  $d_i(k)$  representing the substrate demand for cell growth.

Interestingly, the linear models have exactly the same structure and contains only a few parameters. The only kinetic parameter is  $\gamma$ , which is an image of the cell growth rate. A controller is now designed in order to reject the disturbance  $d_i(k)$ . To this end, the controller will include an on-line parameter estimation procedure so as to track the correct value of  $\gamma$  (which varies as the cell metabolism changes during a culture). The controller will also be made robust to uncertainties in the gain  $b$ , as well as to neglected high frequency dynamics (recall that we have neglected the glucose dynamics, which is not valid at the bioreactor startup).

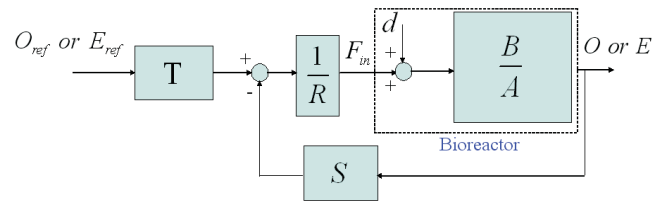


Fig. 2. Closed-loop control of the bioreactor model where  $B$ ,  $A$ ,  $R$ ,  $S$  and  $T$  are polynomials in backward-shift operator  $q^{-1}$ .

### III. SIMPLE DESIGN OF AN ADAPTIVE ROBUST CONTROLLER

#### A. RST Controller

A two-degree-of-freedom RST controller is designed to reject the disturbance and to regulate the output concentration ( $y(k) = O(k)$  or  $E(k)$ ) at the chosen setpoint  $r(k)$ ; see Fig. 2 where  $A(q^{-1}) = 1 - a q^{-1}$  and  $B(q^{-1}) = b q^{-1}$ .

The control law can be written as

$$R(q^{-1}) F_{in}(k) = -S(q^{-1}) y(k) + T(q^{-1}) r(k) \quad (14)$$

and, omitting the backward-shift operator for the sake of clarity, the closed-loop equation takes the form

$$y(k) = \frac{B T}{A R + B S} r(k) + \frac{B R}{A R + B S} d_i(k) \quad (15)$$

Following the internal model principle [12], the unstable pole of the disturbance  $d_i$  (13b) should be included into the  $R$  polynomial, i.e.,  $D = 1 - \gamma q^{-1}$  is a factor of  $R$  which can be written in the form  $R = R' (1 - \gamma q^{-1})$ .

The  $R'ST$  controller polynomials are then computed using a pole-placement procedure [13], in which the reference model is given by

$$H_m(q^{-1}) = \frac{B(q^{-1}) A_m(1)}{B(1) A_m(q^{-1})} \quad (16)$$

The poles of  $A_m(q^{-1})$  are chosen in order to impose the tracking behavior.

The controller polynomials are found by solving a diophantine equation of the form

$$A D R' + B S = A_0 A_m \quad (17)$$

where  $A_0$  is the observer polynomial, which can be selected so as to confer some robustness to the controller.

By replacing the closed-loop transfer function denominator and  $R$  by their new expressions and the disturbance  $d_i(k)$  by (11b) in (15), we obtain :

$$y(k) = \frac{B T}{A_0 A_m} r(k) + \frac{B D R'}{A_0 A_m} \frac{c}{D} \delta(k) \quad (18)$$

The disturbance polynomial  $D$  is compensated (assuming that we have a good knowledge about  $\gamma$ ), and the polynomial  $T$  is chosen so as to ensure setpoint tracking (whose

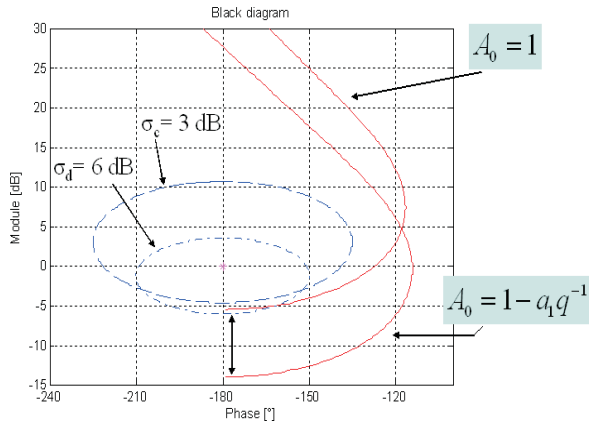


Fig. 3. Robust behavior analysis of the proposed controller in the Black-Nichols diagram

dynamics is specified by polynomial  $A_m$ ) independently of loop robustification (defined by polynomial  $A_0$ ) :

$$T = A_0 \frac{A_m(1)}{B(1)} \quad (19)$$

The biological reactions occur on such a time scale that  $T_s = 0.1h$  is an acceptable sampling period and a first-order tracking behavior with a time constant of  $1h$  can be selected, which corresponds to  $A_m = 1 - 0.9q^{-1}$ .

The tuning of  $A_0$  is achieved by loop-shaping, i.e., by modifying the shape of the corrected open-loop transfer function in the Black-Nichols diagram represented in Fig. 3.

It is well-known that ensuring a modulus lower than 6 dB for the direct sensitivity function  $\sigma_d$  and lower than 3 dB for the complementary sensitivity function  $\sigma_c$  provides a good stability robustness. Those criteria are not respected without robustification ( $A_0 = 1$ ) but a first-order observer polynomial ( $A_0 = 1 - a_1 q^{-1}$ ) is sufficient to ensure a good robustification (Fig. 3). Indeed, the comfortable gain margin confirms the robust behavior at high frequencies, corresponding to the frequency range of the neglected glucose dynamics. By trial and error, we fix the value of the pole  $a_1$  to 0.7.

#### B. Adaptation scheme

As explained in the previous section, the disturbance  $d_i$  can be perfectly canceled out only if the parameter  $\gamma$  is correctly estimated. After the initial time, equation (13b) can be written :

$$d_i(k) - \gamma d_i(k-1) = 0 \quad (20)$$

This equation represents a linear regression which can be solved on-line by a *Recursive Least Squares* algorithm as described in [13].

The adaptation of the gain  $b$  is more straightforward. Indeed, the volume occurring in Table I can be estimated by integration of the feed rate  $F_{in}$  or by direct measurement, if the bioreactor is equipped with a weighting device. The expression of  $b$  is then simply updated.

#### C. Model improvements

We observed experimentally [7] that the ethanol signal does not respond instantaneously to feed rate variations, but display a latency phase estimated between 6 and 12 min. A first model refinement would amount to include a delay of 1 or 2 sampling periods (recall that we have selected a sampling period of 6 min). With a relatively large sampling time, the ethanol probe dynamics can be neglected. However, reducing the sampling intervals can be interesting to get faster updates of the parameter  $\gamma$  and in turn, more effective disturbance rejection. In this case, modeling the ethanol probe dynamics can be achieved by a first-order transfer function with a time constant  $T_{mes}$  (which, depending on the probe, can be in the range 1 – 3 min).

If we include these two refinements into our model, the discrete equivalent model becomes :

$$H(q^{-1}) = \frac{b q^{-3} [(T_s + T_{mes}(v-1)) + (T_{mes} - v(T_s + T_{mes}))q^{-1}]}{(1 - q^{-1})(1 - v q^{-1})} \quad (21)$$

where  $v = e^{(-\frac{T_s}{T_{mes}})}$

#### IV. SIMULATIONS

The results of four simulation runs are presented in this section. The first one considers the regulation of the dissolved oxygen concentration using the appropriate linearized model, the theoretical values of the yield coefficients and kinetic parameters taken from the model of Sonnleitner [1] and the RST controller described in Sections III-A and III-B. The chosen value for  $k_5$  is 0.397 and the initial and operating conditions are as follows :  $k_L a = 50 h^{-1}$  ;  $G_{in} = 350 g/l$  ;  $X_0 = 0.4 g/l$  ;  $G_0 = 0.012 g/l$  ;  $E_0 = 0.9 g/l$  ;  $V_0 = 6.8 l$  ;  $O_0 = 100 \%$  ;  $T_s = 6 min$ . The polynomials  $A_m$  and  $A_0$  are as described in the previous section and the controller polynomials are computed using (17) and (19).

Fig. 4 shows the evolution of the dissolved oxygen concentration ( $O$ ) and the feed flow rate ( $F_{in}$ ). During the first hours, a linear profile is imposed to  $F_{in}$  until  $O$  reaches its setpoint. Then, the controller starts regulating  $O$  at 20 %. After 38 h, a setpoint of 30 % is imposed in order to test the tracking performance, which appears quite satisfactory. Indeed, the dissolved oxygen concentration reaches its new setpoint within a few hours according to the tracking behavior imposed by the reference model (16).

Let us define the productivity of a batch as the ratio between the biomass yield [7] and the batch time  $t_f$  :

$$Y_x = \frac{1}{t_f} \frac{V(t_f) X(t_f) - V_0 X_0}{S_{in} (V(t_f) - V_0)} \quad (22)$$

where the signs 0 and  $f$  indicate the initial and final times.  $Y_x$  is expressed in gram of biomass per gram of glucose per hour :  $g/g/h$

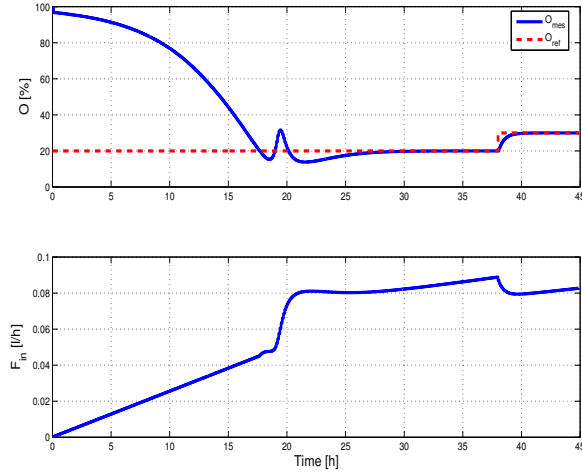


Fig. 4. Simulation results with the RST controller of (III-A). Evolution of the dissolved oxygen concentration ( $O$  : continuous line and  $O_{ref}$  : dashed line) and the feed flow rate ( $F_{in}$ ).

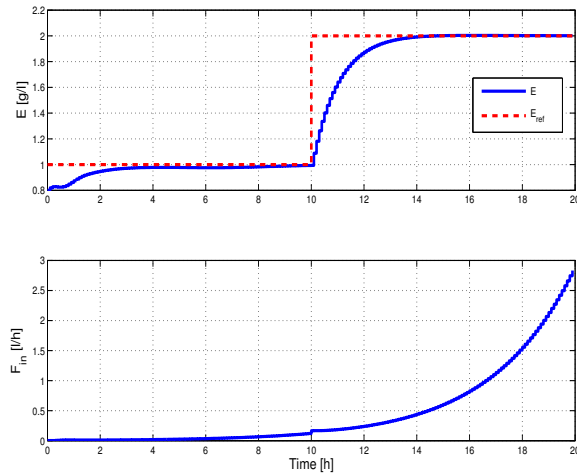


Fig. 5. Simulation results with the RST controller of (III-A). Evolution of the ethanol concentration ( $E$  : continuous line and  $E_{ref}$  : dashed line) and the feed flow rate ( $F_{in}$ ).

For this first simulation, the productivity estimated by (22) amounts to  $0.011 \text{ g/gh}$  after  $45 \text{ h}$ .

The second simulation run illustrates the ethanol regulation with the corresponding linearized model, theoretical parameter values taken from Sonnleitner's kinetic model and the RST controller based on the basic model (13b). An initial ethanol concentration of  $E_0 = 0.8 \text{ g/l}$  is chosen so that the process has to operate in the respiro-fermentative regime, and the only yield coefficient whose knowledge is *a priori* required, is  $k_4 = 0.48$  (see Eq. (1c) and Table I). The other initial and operating conditions, as well as the tracking and observer polynomials are taken as in the first case study.

Fig. 5 shows the evolution of the ethanol concentration

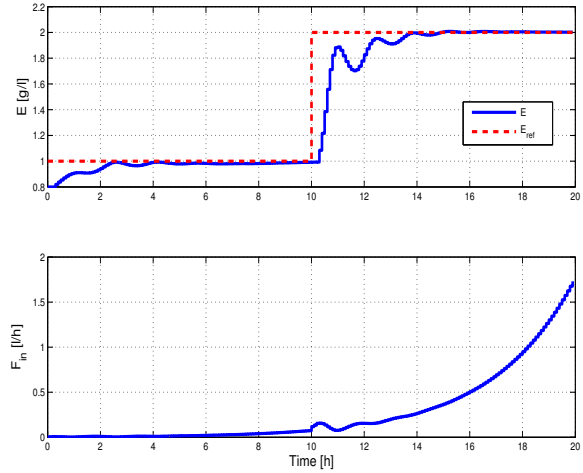


Fig. 6. Simulation results with the RST controller of (III-A) applied to a bioprocess with a time delay. Evolution of the ethanol concentration ( $E$  : continuous line and  $E_{ref}$  : dashed line) and the feed flow rate ( $F_{in}$ ).

( $E$ ) and the feed flow rate ( $F_{in}$ ). The setpoint  $E_{ref} = 1 \text{ g/l}$  is correctly reached after approximately  $8 \text{ h}$  and is maintained until the  $10^{\text{th}}$   $\text{h}$  where the tracking performances are again tested by a step-change to  $2 \text{ g/l}$ . This new setpoint is reached within the next  $4 \text{ h}$  confirming the good tracking behaviour. The productivity of this second batch amounts to  $0.024 \text{ g/gh}$ , which is more than twice the productivity of the first batch. However, this control strategy requires the use of an ethanol probe which is not always available for reasons explained in the introduction. As an alternative to a hardware sensor, a software sensor could be used advantageously [7].

The third test considers the performance of the ethanol regulation designed previously when faced to a process model incorporating a delay of  $12 \text{ min}$ . In this case, the regulation has not been designed taking the delay into account, and the tracking performance are affected by oscillations, as shown in Fig. 6.

The fourth test is based on the somewhat more sophisticated model discussed in Section III-C, which takes the process time delay into account, and a smaller sampling period  $T_s = 1.5 \text{ min}$ . The same initial and operating conditions are used. The higher-order system transfer function requires a new design of the observer polynomial  $A_0$  following the guidelines given in Section III-A and illustrated by Fig. 3. In this particular case, a first-order observer polynomial does not provide enough robustness to the system but a second-order polynomial does.  $A_0 = (1 - 0.9q^{-1})(1 - 0.95q^{-1})$  is consequently chosen.

The evolution of the ethanol concentration and the feed flow rate are represented in Fig. 7. This time, after only  $2 \text{ h}$  the ethanol concentration reaches the setpoint of  $1 \text{ g/l}$ , which is imposed during the first  $10 \text{ h}$ . Then, a step-change to  $2 \text{ g/l}$  is applied in order to assess the tracking performance and the beneficial effect of a faster sampling rate. Again,  $2 \text{ h}$  are sufficient to reach this new setpoint. This quicker response

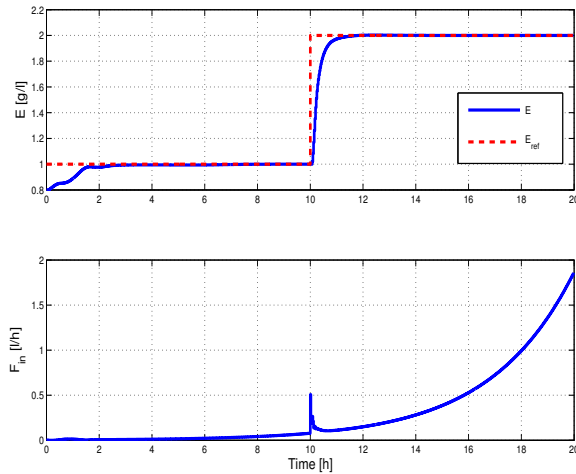


Fig. 7. Simulation results with the RST controller of (III-A) completed by the improvements of (III-C). Evolution of the ethanol concentration ( $E$  : continuous line and  $E_{ref}$  : dashed line) and the feed flow rate ( $F_{in}$ ).

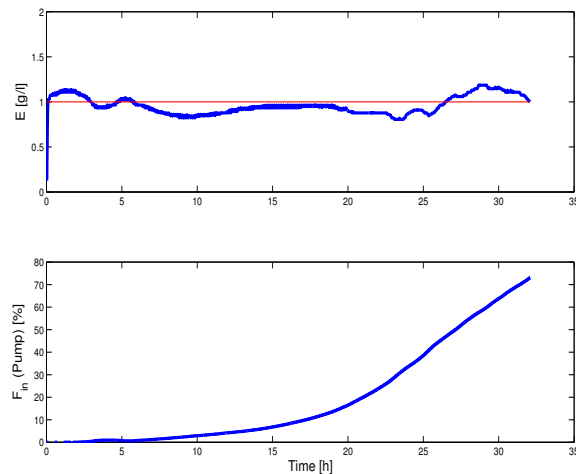


Fig. 8. Experimental results of the ethanol regulation applied to fed-batch cultures of *S. cerevisiae*. Evolution of the ethanol concentration  $E$  (g/l) around  $E_{ref} = 1$  g/l and feed flow rate  $F_{in}$  expressed in % of the maximal pump speed.

does not improve the batch productivity significantly, but provides better tracking and rejection performance.

## V. EXPERIMENTAL RESULTS

The aim of this section is to test experimentally the third control scheme, which appears as the winner of our simulation tests. Fed-batch cultures of *S. cerevisiae* have been performed with a laboratory-scale 20-liter bioreactor and experimental results are shown in Figs. 8 and 9.

For these experimental tests, only a 2-sampling-period delay has been taken into account. A sampling period of 6 min is chosen so that the ethanol probe dynamics can be neglected.

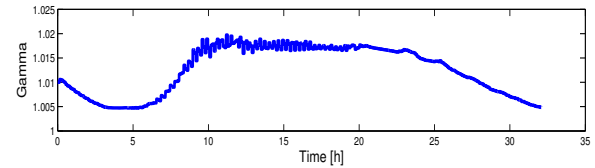


Fig. 9. Experimental results of the ethanol regulation applied to fed-batch cultures of *S. cerevisiae*. Evolution of the parameter  $\gamma$  image of the cells growth rate.

Fig. 8 shows the evolution of the ethanol concentration and the feed flow rate expressed as a percentage of the maximum pump speed. The ethanol concentration stays around the setpoint  $E_{ref} = 1$  g/l during the first 10 h and then follows it almost exactly for the next 10 h. Actually, the first hours correspond to the adaptation of the  $\gamma$  parameter represented in Fig. 9. When the estimate converges, the regulation of the ethanol concentration becomes more accurate (as the disturbance, which represents the substrate demand for cell growth, can be compensated almost exactly).

After 20 h, the ethanol concentration deviates slightly from the setpoint. This can be explained by an apparent decrease of the cell growth as reflected by the estimated value of  $\gamma$ . This limitation phenomenon can be due to a lack of some nutriment in the culture medium. Indeed, cell growth is so efficient that the culture medium is exhausted after a certain batch time. After this time, the feed flow rate evolution becomes linear as  $\gamma$  decreases. Despite this deviation, the controller maintains  $E$  around 1 g/l and prevents it from moving too far from the setpoint. This demonstrates the efficiency of the tracking control even in the presence of unexpected or unknown phenomena like the observed limitation.

This control strategy has been applied to different (genetically manipulated) strains of *S. cerevisiae* bioreactors, yielding similar performance. This series of experimental tests demonstrates the reliability of the controller in various experimental conditions. The productivity gain, as compared to standard practice (open-loop bioreactor operation with sub-optimal feeding profile) can be estimated to about 40 %.

## VI. CONCLUSION

Based on singular perturbation and linearization, three simple linear models are derived, which describe the transfer between the feed rate and the dissolved oxygen concentration or the ethanol concentration, respectively. In the latter case, two different linear models are used to describe the respirative and respiro-fermentative mode of operation. Interestingly, these three linear models have exactly the same structure, and only differ in the values of their coefficients so that the same controller design procedure can be used.

An adaptive RST controller is then designed to regulate the dissolved oxygen or the ethanol concentrations, according to the considered model, at an imposed setpoint. This design is based on pole placement (for setpoint tracking) and the

selection of an observer polynomial (for loop robustification), which can be achieved independently.

The performance of these control schemes is then assessed both in simulation and in real experimental studies with different yeast strains. Attention is focused on ethanol regulation, which leads to better biomass productivity than oxygen regulation. Ethanol can be either measured directly using an appropriate probe, or indirectly using a software sensor based on elementary signals such as base addition (for pH control), stirrer rotational speed, etc. [7].

In all the case studies, the controller performed well, demonstrating its reliability under various conditions. As compared to conventional open-loop operation, the application of the control schemes can lead to about 40 % productivity gain.

#### Acknowledgements

This paper presents research results of the Belgian Network DYSCO (Dynamical Systems, Control, and Optimization), funded by the Interuniversity Attraction Poles Programme, initiated by the Belgian State, Science Policy Office. The scientific responsibility rests with its author(s). The support of the Walloon Region in the framework of the COCA project (DGTRE) is also gratefully acknowledged.

#### REFERENCES

- [1] B. Sonnleitner and O. Käppeli, "Growth of *Saccharomyces cerevisiae* is controlled by its limited respiratory capacity : Formulation and verification of a hypothesis," *Biotechnol. Bioeng.*, vol. 28, pp. 927–937, 1986.
- [2] J. Axelsson, "On the role of adaptive controllers in fed-batch yeast production." Copenhagen : ADCHEM 1988, Aug 1988.
- [3] Y. Pomerleau, "Modélisation et commande d'un procédé fed-batch de culture des levures pain," Ph.D. dissertation, Département de génie chimique. Université de Montréal., 1990.
- [4] Y. Pomerleau and G. Viel, "Industrial application of adaptive nonlinear control for bakers' yeast production." Keystone, CO, USA : ICCAFT 4, March 1992.
- [5] L. Chen, G. Bastin, and V. van Breusegem, "A case study of adaptive nonlinear regulation of fed-batch biological reactors," *Automatica*, vol. 31, no. 1, pp. 55–65, 1995.
- [6] S. Valentinotti, B. Srinivasan, U. Holmberg, D. Bonvin, C. Cannizzaro, M. Rhiel, and U. von Stockar, "Optimal operation of fed-batch fermentations via adaptive control of overflow metabolite," *Control engineering practice*, vol. 11, pp. 665–674, 2003.
- [7] F. Renard, A. Vande Wouwer, and M. Perrier, "Robust adaptive control of yeast fed-batch cultures," *ADCHEM 2006, Brazil*, April 2006.
- [8] M. Akesson, "Probing control of glucose feeding in *escherichia coli* cultivations," Ph.D. dissertation, Lund Institute of Technology, 1999.
- [9] L. de Mar, L. Andersson, and P. Hagander, "Probing control of glucose feeding in *vibrio cholerae* cultivations," *Bioprocess Biosyst.*, vol. 25, pp. 221–228, 2003.
- [10] X. Hulhoven, F. Renard, S. Dessoy, P. Dehottay, P. Bogaerts, and A. Vande Wouwer, "Monitoring and control of a bioprocess for malaria vaccine production," *5th IFAC Symposium on Robust Control Design*, July 2006.
- [11] S. Valentinotti, C. Cannizzaro, B. Srinivasan, and D. Bonvin, "An optimal operating strategy for fed-batch fermentations by feeding the overflow metabolite." Hong Kong : ADCHEM 2004, 2004.
- [12] B. A. Francis and W. M. Wonham, "The internal model principle of control theory," *Automatica*, vol. 12, pp. 457–465, 1976.
- [13] K. J. Astrom and B. Wittenmark, *Computer Controlled Systems Theory and Design*. Information and System Sciences. Prentice Hall, 1997.